A Monte Carlo study of scaling and universality in 2D directed percolation

1984 J. Phys. A: Math. Gen. 17 2651

(http://iopscience.iop.org/0305-4470/17/13/017)

J. Phys. A: Math. Gen. 17 (1984) 2651–2665. Printed in Great Britain

A Monte Carlo study of scaling and universality in 2D directed percolation

J Benzoni

Department of Physics, University of California, Santa Barbara, California 93106, USA

Received 27 March 1984

Abstract. Monte Carlo data for the pair correlation function is obtained on five different lattices for the directed percolation problem in two dimensions. Scaling is tested and found to hold beyond 20 lattice spacings for all models. Evidence is found to support the universality of the scaling function. The values of the exponents $\gamma/\nu_{\parallel}$ and $\nu_{\perp}/\nu_{\parallel}$ are extracted from the data; our results for all models are summarised by

$$\gamma/\nu_{\parallel} = 1.305 \pm 0.007$$

and

$$\nu_{\perp}/\nu_{\parallel} = 0.629 \pm 0.010.$$

Comparison is made with estimates derived by other means.

1. Introduction

In ordinary percolation sites or bonds are filled at random with probability p. Percolation then proceeds along paths between occupied nearest-neighbour links and the orientation of a link is not restricted in either direction along any axis. A variant of this model is directed percolation in which sites or bonds are also filled at random with probability p, but nearest-neighbour links must be oriented such that percolation is allowed to proceed in only one direction along the axis which is designated as the preferred direction. It is sensible then to associate this axis with time and therefore percolation proceeds in the direction of increasing time. In this sense time reversal symmetry is broken in directed percolation.

The effect of this preferred direction can be observed if one looks at the shape of typical clusters in each model. The clusters formed by collections of nearest-neighbour links in ordinary percolation are isotropic. At $p = p_c$ a fractal structure is formed. In directed percolation the clusters for $p < p_c$ take on a characteristic shape in which the size of the clusters in the preferred direction is characterised by a different length scale from that in the perpendicular directions. Cluster growth in the preferred direction is restricted to that of increasing time but in the perpendicular directions growth may be isotropic.

The pair connectedness or pair correlation function $G(\boldsymbol{r}_2, \boldsymbol{r}_1)$ is a measure of the probability that sites $\boldsymbol{r}_2$ and $\boldsymbol{r}_1$ are connected by some path irrespective of the other sites in the lattice. Lines of constant G give the average shape of a cluster. In directed percolation $\boldsymbol{r}_i = (\boldsymbol{x}_i, t_i)$ and we have the added restriction that $t_2 > t_1$ for G to be non-zero. This corresponds to a Markov process, since the probabilities $G(\{\boldsymbol{x}_i\}, t)$ that a given

set of sites $\{x_i\}$ are connected to the origin are related in a direct way to the probabilities $G(\{x_i\}, t-1)$. Such models arise in chemistry and biology (Schlögl 1972) and population dynamics (Griffeath 1979, Murray 1979).

Cardy and Sugar (1980) have shown that directed percolation is in the same universality class as Reggeon Field Theory (RFT) near five dimensions. The scaling law for G that one obtains from RFT (Abarbanel *et al* 1976) but written in statistical mechanics notation is

$$G(\boldsymbol{x}, t) \sim |p-p_c|^{2\beta}\psi(|p-p_c|^{2\nu_\perp}r^2, |p-p_c|^{\nu_\parallel}t) \tag{1.1}$$

where β, $\nu_\parallel$ and $\nu_\perp$ are critical exponents which depend only on the number of transverse dimensions D (where $D=d-1$) and ψ is a universal scaling function calculable within the ε expansion. Noting that the correlation lengths $\xi_\perp$ and $\xi_\parallel$ for the directions perpendicular and parallel to the preferred direction, respectively, are given asymptotically by

$$\xi_\perp \sim |p-p_c|^{-\nu_\perp}, \qquad \xi_\parallel \sim |p-p_c|^{-\nu_\parallel}, \tag{1.2}$$

we find that G can be written in terms of another scaling function (Φ) for p exactly at the critical probability p_c:

$$G(\boldsymbol{x}, t) \sim At^{-2\beta/\nu_\parallel}\Phi(B\boldsymbol{x}/t^{\nu_\perp/\nu_\parallel}). \tag{1.3}$$

Here, as in (1.1), $\boldsymbol{x}=\boldsymbol{x}_2-\boldsymbol{x}_1$, $t=t_2-t_1$ and A and B are non-universal constants.

A hyperscaling relation between exponents written in RFT notation is (Cardy and Sugar 1980)

$$\beta = \tfrac{1}{2}\nu(\tfrac{1}{2}Dz-\eta). \tag{1.4}$$

The set of exponents β, η, z and ν are also used in the Reggeon quantum spin (RQS) model (Amati *et al* 1976, Brower *et al* 1978) which is believed to be in the same universality class as RFT. In statistical mechanics β corresponds to the percolation probability exponent, γ corresponds to the mean size exponent and the hyperscaling relation (1.4) becomes (Essam and De'Bell 1983)

$$\beta = \tfrac{1}{2}(D\nu_\perp + \nu_\parallel - \gamma). \tag{1.5}$$

The exponents η, z and ν in RFT and RQS and the exponents γ, $\nu_\parallel$ and $\nu_\perp$ in statistical mechanics are related by

$$\eta = \gamma/\nu_\parallel - 1 \qquad z = 2\nu_\perp/\nu_\parallel \qquad \nu = \nu_\parallel. \tag{1.6}$$

The exponents η, z and ν have been calculated in RFT near $d=5$ and the results taken over to this model, but to lowest order in ε they are not expected to be accurate near $d=2$.

In $d=2$ Brower *et al* (1978) calculated the exponents η, z and ν in the RQS model using a high-temperature expansion. Grassberger and De La Torre (1979) used Monte Carlo methods in a lattice version of RFT and thereby calculated η, z and ν. By direct enumeration Blease has calculated β and γ (1977a) and γ and $\nu_\parallel$ (1977b) for directed percolation, but could not infer $\nu_\perp$ in either work since the hyperscaling relation (1.5) was not obtained until after these works were completed. Kertesz and Vicsek (1980) used Monte Carlo means to obtain ν_0, but assumed only one correlation length for the system and therefore did not calculate $\nu_\perp$ nor $\nu_\parallel$. Dhar and Barma (1981) also used Monte Carlo methods and obtained β and γ. Kinzel and Yeomans (1981) used a transfer matrix approach to obtain $\nu_\parallel$ and $\nu_\perp$. Essam and De'Bell (1983) estimated

γ and then obtained $\nu_{\parallel}$ and $\nu_{\perp}$ by direct enumeration. Table 1 gives a summary of the exponents calculated in this work and by other authors and also gives an estimate of their respective errors.

In this work we use Monte Carlo methods to create ensembles of clusters on the directed lattice and thereby infer the pair connectedness function G at $p = p_c$. Plots are then made of the normalised scaling function to observe the onset of scaling. Scaling is tested by plotting the scaling function (Φ) against the scaling variable (z) for different values of time (the preferred direction on the lattice). This scaling function has not been shown in other works to be universal; by comparing plots of the scaling function for different models (suitably normalised) in two dimensions ($D = 1$), we check the universality of the scaling function. Another more quantative test of universality which we use in this work is a comparison of certain ratios of the moments of the scaling function computed for each model. These results, accurate to within 5%, also suggest that universality is obeyed. Finally, by plotting the log of the moments of the pair connectedness function against the log of the time, we obtain estimates of the critical exponents which we compare to those calculated by other means.

2. Monte Carlo data

It is a relatively simple task to generate Monte Carlo data for the pair connectedness function $G(x, t)$, if one views this function at each step in time as a measure of the existence of a generation in a population. That is, the function $G(x, t)$ is a measure of the probability that an individual at the origin has a descendent at position x in generation t. The process of generating the evolution of a population (from which $G(x, t)$ is derived) is simplified by the Markovian nature of the problem. That is, the existence of a member of any given generation is dependent upon the existence of its immediate predecessors in the previous generation. The random nature of the problem is characterised by the parameter p. Note that for $p < p_c$ the population is ultimately doomed to extinction even though it may experience several generations of sustained size and even growth before its eventual demise. The value of p at which the destiny of the population goes from certain demise to a finite probability for infinite growth defines p_c.

To fix ideas, consider site percolation on the square lattice at $p = p_c$. To determine whether an individual in a particular generation exists, that is, if the site (x, t) is occupied, we must first ask whether its immediate predecessors exist, that is, whether either of the two sites $(x+1, t-1)$ or $(x-1, t-1)$ are occupied. If one or both ancestors exist, then the probability that individual (x, t) exists is p_c. This occurs irrespective of all other individuals in generation t. If neither ancestor exists, then the individual (x, t) cannot exist. That is, individual (x, t) cannot spontaneously exist but must have at least one ancestor. This is an expression of the percolative nature of the problem. Since this process occurs for every generation succeeding from the origin, the only individuals (sites) considered in evaluating $G(x, t)$ are those whose ancestry can be traced back to the origin. In this sense, $G(x, t)$ is the probability that an individual exists at x in generation t by some geneaology, irrespective of other members of that generation.

In the bond percolation problem as expressed in terms of population dynamics, we consider all individuals in all generations to exist, that is, all sites are present with probability one. The correlation function $G(x, t)$ in this case is again the probability

Table 1. Exponents and critical probabilities (p_c) from this work and various other sources (including errors).

	A	B	C	D	E	F	G
P			0.643 ± 0.002[1] 0.6446 ± 0.0002[2] 0.6445 ± 0.0005[3] 0.632 ± 0.004[4] 0.644 ± 0.001[5] 0.6446 ± 0.0002[6]	0.479 ± 0.003[1] 0.4774 ± 0.0004[2] 0.465 ± 0.015[4] 0.4777 ± 0.0005[7]	0.7058 ± 0.0001[5] 0.7055 ± 0.0005[7]	0.5949 ± 0004[7]	0.8228 ± 0.0001[5]
γ			2.26 ± 0.07[1] 2.27 ± 0.016[2] 2.19 ± 0.03[3] 2.269 ± 0.018[7]	2.35 ± 0.09[1] 2.27 ± 0.04[2]			
$\nu_{\parallel}$	1.691 ± 0.018[9]	1.736 ± 0.001[9]	1.730 ± 0.009[2] 1.65 ± 0.06*[7] 1.739 ± 0.002[5] 1.733 ± 0.013[6] 1.730 ± 0.015[7]	1.70 ± 0.05[2] 1.71 ± 0.025[7]	1.730 ± 0.002[5] 1.715 ± 0.015[7]	1.70 ± 0.002[5]	1.732 ± 0.003[5]
$\nu_{\perp}$			1.099 ± 0.001[5] 1.098 ± 0.006[6] 1.095 ± 0.008[7]	1.095 ± 0.009[7]	1.094 ± 0.001[5] 1.095 ± 0.007[7]	1.084 ± 0.009[7]	1.095 ± 0.002[5]
$(\gamma/\nu_{\parallel}) - 1$	0.314 ± 0.007[9]	0.317 ± 0.002[8]	0.313 ± 0.016[2] 0.312 ± 0.022[7] 0.305 ± 0.004[10]	0.34 ± 0.027[2] 0.302 ± 0.004[10]	0.312 ± 0.004[10]	0.297 ± 0.004[10]	0.306 ± 0.004[10]
$\nu_{\perp}/\nu_{\parallel}$	0.637 ± 0.004[9]	0.636 ± 0.007[8]	0.6321 ± 0.0004[5] 0.633 ± 0.002[6] 0.633 ± 0.010[7] 0.630 ± 0.006[10]	0.640 ± 0.015[7] 0.618 ± 0.007[10] 0.640 ± 0.007[10]	0.6365 ± 0.0004[5] 0.639 ± 0.010[7]	0.638 ± 0.012[7] 0.621 ± 0.006[10]	0.6321 ± 0.0004[5] 0.636 ± 0.007[10]
β			0.29 ± 0.01[1] 0.276 ± 0.014[3] 0.278 ± 0.005[7]	0.28 ± 0.02[1]			

Models: A = Reggeon field theory, B = Reggeon quantum spin, C = square bond, D = triangular bond, E = square site, F = triangular site, G = square site-bond.
[1] Blease (1977a), [2] Blease (1977b), [3] Dhar and Barma (1981), [4] Kertesz and Vicsek (1980), [5] Kinzel and Yeomans (1981), [6] De'Bell and Essam (1981), [7] De'Bell and Essam (1983), [8] Brower *et al* (1978), [9] Grassberger *et al* (1979), [10] Benzoni (this work).

that an individual at (x, t) is descended from the individual at the origin, but now it is the specific relations (bonds) between generations which are important. As in the site problem, to determine if an individual is part of this family tree, we must first ask if its immediate ancestors are part of the family tree. If neither ancestor is descended from the origin, then the individual at (x, t) cannot be descended from the origin. If one or both ancestors are descended from the origin, then there is some probability that (x, t) is too. Clearly an individual at (x, t) has a greater chance of being a descendent of the individual at the origin if both its ancestors are descended from the origin, since in that case there are two possible ways in which the individual can be related to the origin. An example of each of these types of sites is shown in figure 1.

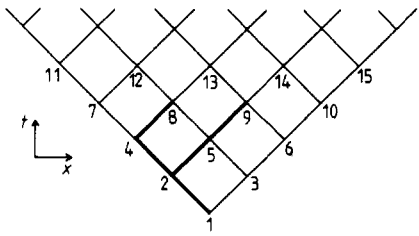

Figure 1. A typical population evolved through three generations. Sites 11 and 15 have probability zero of being related to the origin, sites 12 and 14 have probability p_c of being related to the origin and site 13 has probability $2p_c - p_c^2$ of being related to the origin. Site 13 has a greater probability of being connected to the origin, since both of its ancestors (sites 8 and 9) are connected to the origin.

The Markovian nature of directed percolation makes calculation of $G(x, t)$ simpler than in the case of ordinary percolation, since in tracing these ancestral paths one is allowed to move only backward in the preferred or time direction. This greatly restricts the number of possible paths which connect a site at (x, t) to the origin.

Following this Markovian idea, that an individuals existence at any site (x, t) is solely dependent upon the existence of its predecessors in generation $t-1$, we constructed an algorithm to generate Monte Carlo data of $G(x, t)$. Number the sites in the lattice in order of increasing position (x) and increasing time (t). Mark these sites with an index (i). Create the arrays GI, GTOT and GSQ which are labelled by the site numbers (i). These arrays contain N elements where N is related to the total or maximum number of time steps T by $N = \frac{1}{2}(T+1)(T+2)$. Note that the origin is defined as $t = 0$ and therefore N is written in terms of $T+1$. The array GI contains the occupation numbers for a single population evolution and hence contains only 'zeros' (if a site is vacant) and 'ones' (if a site is occupied). Note that site 1 (the origin) is always occupied, and so GI always has a one as its first element (GI(1) = 1). The array GTOT contains the cumulative data for all such evolutions. The array GSQ, used for statistics purposes, contains cumulative data for the sum of squares of bins of data.

To determine if site i (corresponding to (x, t)) is occupied, check its predecessors on row $t-1$ for occupancy. Form the sum of the occupation numbers of the ancestors of (x, t) which are contained in GI. In the case of bond percolation on the square lattice, apply the following rules to this sum:

(1) If sum = 0 then GI(i) = 0 with probability one.

(2) If sum = 1 then GI(i) = 1 with probability p_c. To this end we compare a random number to p_c. If the random number is greater than p_c, GI(i) = 0. If the random number is less than p_c, GI(i) = 1.

(3) If sum = 2 then GI(i) = 1 with probability $2p_c - p_c^2$. Compare a random number to $2p_c - p_c^2$. If the random number is greater than $2p_c - p_c^2$, GI(i) = 0. If the random number is less than $2p_c - p_c^2$, GI(i) = 1.

These rules change only slightly for other types of percolation. For example in site percolation on the square lattice, if both ancestor sites are occupied (sum = 2) then GI(i) = 1 with probability p_c rather than $2p_c - p_c^2$.

Using these algorithms we generated data for five models in two dimensions ($D = 1$): square bond, triangular bond, square site, triangular site and square site–bond. In the site–bond model, the simple case where both sites and bonds are present with the same probability p was used, since p_c for this model is readily available (Kinzel and Yeomans 1981). After preliminary runs to determine the point at which scaling sets in, at least two runs of each model were made in which the maximum time step was taken as $T = 60$. This value of T is much greater than that used by researchers using direct enumeration schemes (Blease 1977a, b, Essam and De'Bell 1981, 1983). In those works $T \leqslant 15$ and corrections to scaling are likely to be important. Kinzel and Yeomans (1981) use a transfer matrix approach on an infinitely long strip, but again the width of the strip is about 15 lattice spacings and so care must be taken in treating finite size effects. A direct comparison cannot be made with the work of Brower *et al* (1978) but they also rely upon an extrapolation to asymptotically large times. In this work we observe scaling only for $t \geqslant 20$ and therefore corrections to scaling were not considered as an important source of error. Since we do not rely upon extrapolation to asymptotically large times the finite size effects resulting from the upper bound were neglected.

At least one run of each model with ensemble size 10 000 and one run each with ensemble size 50 000 was made. These programs, run on a VAX 11/780, had CPU times of approximately 1 hour and 10 hours respectively. The differences in ensemble size and the disparity in CPU time are due to the manner in which statistics were obtained which will be explained later in this paper. The results obtained for the ensemble averaged occupation numbers $G(x, t)$, for the first few sites are in agreement with the predictions made by direct enumeration (to within the statistical error expected for uncorrelated Gaussian distributed events). The values of p_c used for each model were taken from data obtained by direct means and appear in table 1.

The validity of these values of p_c was not tested in this work. The central values of p_c reported from direct means were taken as fixed. Since these programs do not depend on running to asymptotically large times the effects of errors in p_c in the calculation of the exponents should not be significant. That scaling is exhibited (which is discussed later in this paper) demonstrates that this is true.

To obtain an estimate of the statistical errors incurred in our data, we consider each run to be uncorrelated with all other runs. This is strictly true in the limit where the random number generator is truly random, i.e. where the period of correlations is infinite. Since machine generated random numbers have some finite period (albeit large) our measurements must either be made well within this period or some other computational tricks must be used. The relatively small run size insures that the former is true. Then, if the occupation number at each site is independent of all other sites, the ensemble averaged occupation number ($G(x, t)$) is expected to be a Gaussian distribution about some average value. The square root of the sample variance (σ^2) of $G(x, t)$ at any site (x, t) is a measure of the error in $G(x, t)$ at that site. To compute

the sample variance for a set of Gaussian distributed numbers, one needs to calculate a mean and a mean square value for those numbers. To obtain a mean square occupation number for a site, we 'bin' the data from individual runs of GI into equal subsets of those contained in GTOT. That is, at each site i and for each equal subset or bin of the total number of runs in the ensemble, a sum of the occupation numbers from individual runs of GI(i) are kept. The mean value of $G(x, t)$ for that subset and also the mean value squared can then be obtained. The mean squared value is added to the total in GSQ(i). The average of these squared quantities over all bins in the ensemble gives a measure of the mean square value of $G(x, t)$ at each site i. Then the root mean square deviation, a measure of the error in our data for G at each site i, can be found from the square root of the difference of the mean square and the square of the mean.

It is important to note that this type of error analysis is, for data collected at each site i, completely independent of any other site in the lattice, that is, uncorrelated. If G at each site were indeed uncorrelated with every other site, then for calculated quantities involving an integral or sum over G we can expect a standard deviation which goes inversely as the square root of the total number of values of G involved. However, the data obtained for G at time t is dependent upon the data obtained at time $t-1$, since the existence of individuals at time t depends upon the existence of those at time $t-1$ in some way. This introduces an uncertainty into the error analysis of the exponents which cannot be eliminated through some simple manipulation of the data. Grassberger and De La Torre (1979) also cite these correlation effects and use runs above and below p_c in their work as a consistency check. The errors obtained for the exponents from runs with ensemble size 10 000 were calculated in this manner. The errors that one obtains are unrealistically small.

A more accurate measure of the error in calculated quantities can be obtained if they are measured separately for each bin of data. The data for 50 000 runs was handled in this manner. Data was placed into bins of 1000 runs each and the exponents calculated for each bin. This provides 50 independent measurements of the exponents from which we can find the mean and the standard deviation (σ), which is a measure of our statistical errors.

The choice of 1000 runs per bin was made on the basis of keeping errors of the first type (including systematic error) 'small'. That is, the error in calculating an exponent (by least squares fit to a straight line) should be much smaller than the fluctuations of those exponents about their mean. The choice of 50 bins which in turn implies ensembles of 50 000 was made to keep total CPU time minimal. Since the calculated mean is from some (random) sample population (size 50) of the parent population whose mean is the 'true' value which we seek, we would like a measure of the amount that these two differ. Such a measure is provided by the standard deviation (σ) of the sample distribution divided by the square root of the number of points in our sample distribution (50). It is this measure which we have quoted as the errors in our results (table 1).

3. Tests of scaling and universality

To find the onset of scaling we consider the moments of $G(x, t)$ at fixed t. By definition, the nth moment of G is

$$M^{(n)}(t) \equiv \int \mathrm{d}x\, |x|^n G(x, t). \tag{3.1}$$

If the scaling form, (1.3) is correct, then these moments should behave as

$$M^{(n)}(t) \sim A t^{p+(n+1)q} \int \mathrm{d}z\, |z|^n \Phi(Bz) \tag{3.2}$$

where $p \equiv \gamma/\nu_{\parallel} - \nu_{\perp}/\nu_{\parallel} - 1$ and $q \equiv \nu_{\perp}/\nu_{\parallel}$. The integral over the scaling function Φ is just a constant. Therefore if we plot $M^{(n)}(t)/t^{p+(n+1)q}$ against t the plots should like on a straight line and with zero slope in the scaling region. Such a plot with $n = 0, 1, 2$ for square bond percolation is shown in figure 2.

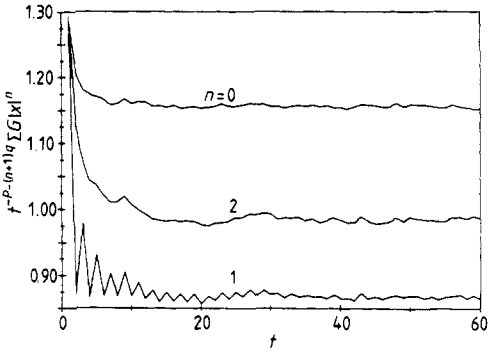

Figure 2. Plots of $M^n(t)/t^{p+(n+1)q}$ against t for square bond percolation.

These plots show that scaling is obeyed for $t \geqslant 20$. This lower bound on scaling is approximately the same for all models tested. This lower bound was used in subsequent calculations involving $t_{\min}$. Note that these plots are sensitive to the values of the exponents used in the powers of p and q. That is, if the power $p+(n+1)q$ to which t is raised is in error by an amount $\delta(n)$, then the plots of $M^n(t)/t^{p+(n+1)q}$ against t will show power law behaviour; this error can occur due to errors in γ, $\nu_{\parallel}$, $\nu_{\perp}$ or combinations of all three. Figure 3 shows the sensitivity of $M^n(t)/t^{p+q}$ for square bond percolation to fluctuations in the exponent $\nu_{\parallel}$ over a range of $\pm 10\%$.

Another visual or graphical test of scaling which is related to the first test is a plot of the scaling function (Φ) against the scaling variable (z) for the same model but different values of time. Figure 4 shows such a plot for square bond percolation. Note that the nth moment of the scaling function at some fixed time equals the normalised nth moment of $G\,(M^n(t)/t^{p+(n+1)q})$ at that time. Define $\chi^{(n)}$ as the nth moment of Φ

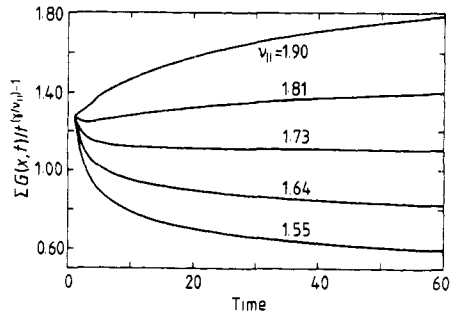

Figure 3. Plot of $M^n(t)/t^{p+q}$ against t for square bond percolation showing the variation of these moments with $\nu_{\parallel}$.

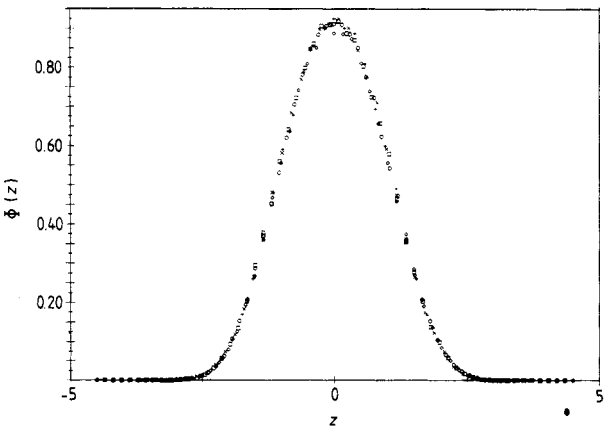

Figure 4. Plots of $\Phi(z)$ against z for square bond percolation at different values of t (+, 40; ×, 45; ◇, 50; □, 55; ○, 60).

at fixed time; combining (1.3) and (3.1) we find for $\chi^{(n)}$

$$\chi^{(n)} \equiv A \int \mathrm{d}z\, |z|^n \Phi(Bz) = \frac{\int \mathrm{d}x\, |x|^n G(x,t)}{t^{p+(n+1)q}} = \frac{M^{(n)}(t)}{t^{p+(n+1)q}}. \tag{3.3}$$

Hence an individual point in one of the plots of $M^{(n)}/t^{p+(n+1)q}$ against t is comprised of an integral over the corresponding moment of Φ. Therefore, we can expect that these plots of the scaling function are not as susceptible to errors in the exponents as are the normalised moments of G. These plots do show however, that the structure of the scaling function is indeed correct.

We have tested universality in 2D directed percolation in several ways. The first and simplest means is a visual test. We plot the scaling function $\Phi(z)$ against the scaling variable (z) for different models on the same graph and observe whether or not the curves lie on top of one another. Of course, the axes must be rescaled since universality asserts only that the functional form of the scaling function is universal, that is

$$A_1 \Phi_1(B_1 z) = \Phi_2(z) \tag{3.4}$$

where the subscripts 1 and 2 can be any 2D directed percolation model. The values of A and B for each model are given in table 2. A plot of the five (rescaled) models which we tested is shown in figure 5. These functions are not strongly susceptible to errors in the exponents for the same reasons as stated in the tests of scaling. The agreement of all five models can be seen to be quite good, suggesting that universality is obeyed.

Table 2. Values of the coefficients A and B for each model tested.

Model	A	B
Square bond	1.0000	1.0000
Triangular bond	0.9611	1.3987
Service site	1.0292	0.8632
Triangular site	1.1279	1.0904
Square site–bond	0.9872	0.9227

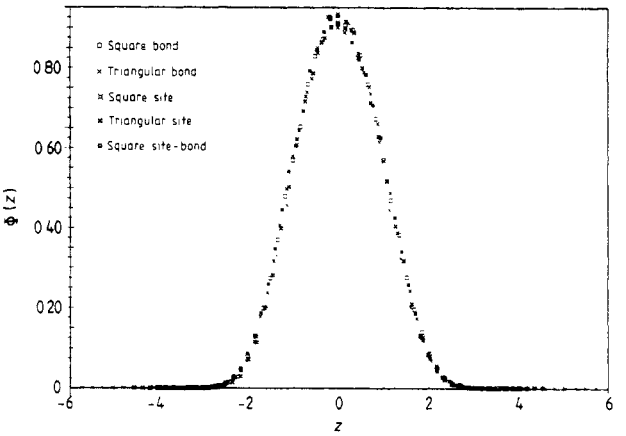

Figure 5. Plots of $A\Phi(z)$ against z/B for all models tested.

A more quantitative test of universality consists of taking ratios of the moments of the scaling function (Φ). Using (10), the nth moment of Φ is given by

$$\chi_i^{(n)} \equiv A_i / B_i^{(n+1)} \int |z|^n \Phi(z)\, dz. \tag{3.5}$$

Then, ratios such as

$$\begin{aligned} &\chi^{(1)^2}/\chi^{(0)} * \chi^{(2)} \equiv C, \qquad &&\chi^{(1)^3}/\chi^{(0)^2} * \chi^{(3)} \equiv D, \\ &\chi^{(1)^4}/\chi^{(0)^3} * \chi^{(4)} \equiv E, \qquad &&\chi^{(2)^2}/\chi^{(0)} * \chi^{(4)} \equiv F, \\ &\chi^{(2)^2}/\chi^{(1)} * \chi^{(3)} \equiv G \end{aligned} \tag{3.6}$$

can be formed for each model, and the constants C, D, E, F, and G should be universal, although obviously not all independent. To test this hypothesis, we computed the moments of Φ using several different integration schemes. The results for the three best independent moment ratios using different integration schemes are shown in table 3. Note that while the scaling function appears to be Gaussian, it must be exponential in the wings. Therefore, these ratios are also taken for a pure Gaussian and a decaying exponential ($\exp(-|x|)$) for comparison.

It can be shown that the ratios of these moments are far less susceptible to errors in the exponents than to statistical fluctuations in the data and errors incurred by the integration scheme itself. To average out statistical fluctuations, the moments $\chi^{(n)}$ were computed for each time from $t = 20$ to $t = 60$ and averaged over these times to obtain $\overline{\chi^{(n)}}$. That is, the values of the normalised moments of G as shown in figure 2 are averaged from $t = 20$ to $t = 60$.

$$\begin{aligned} \overline{\chi^{(n)}} &\equiv \sum_{t=20}^{60} \chi^{(n)} \Big/ \sum_{t=20}^{60} 1 \\ &= \sum_{t=20}^{60} \frac{\int dx\, |x|^n G(x,t)}{t^{p+(n+1)q}} \Big/ \sum_{t=20}^{60} 1. \end{aligned} \tag{3.7}$$

Note that no weighted average over $\chi^{(n)}$ at different times is taken, since the values at lower t have a smaller statistical fluctuation while those at higher t have less error due to corrections to scaling. The values of the exponents used in evaluating these

Table 3. Moment ratios C, D and G (as defined in text) for all models tested and for a Gaussian and decaying exponential as well. Integration by (*a*) Simpson's rule, (*b*) trapezoidal rule, (*c*) square counting.

(*a*) Simpson's Rule

Constant	1	2	3	4	5	6	7	8
C	0.657	0.666	0.662	0.645	0.656	0.657	0.637	0.500
F	0.380	0.394	0.387	0.365	0.379	0.381	0.333	0.167
G	0.814	0.820	0.818	0.809	0.814	0.815	0.785	0.667

(*b*) Trapezoidal Rule

Constant	1	2	3	4	5	6	7	8
C	0.661	0.668	0.665	0.652	0.660	0.661	0.637	0.500
F	0.380	0.394	0.387	0.365	0.379	0.381	0.333	0.167
G	0.812	0.819	0.816	0.805	0.812	0.813	0.785	0.667

(*c*) Square Counting

Constant	1	2	3	4	5	6	7	8
C	0.661	0.668	0.665	0.652	0.660	0.661	0.637	0.500
F	0.380	0.394	0.387	0.365	0.379	0.381	0.333	0.167
G	0.812	0.819	0.816	0.805	0.812	0.813	0.785	0.667

(1) square bond, (2) square site, (3) square site–bond, (4) triangular bond, (5) triangular site, (6) average value of models 1–5, (7) Gaussian, (8) decaying exponential ($\exp(-|x|)$).
Gaussian moments ($M^{(n)}$) $C = 2/\pi$, $F = \frac{1}{3}$, $G = \pi/4$.
Decaying exponential ($\exp(-|x|)$) $C = \frac{1}{2}$, $F = \frac{1}{6}$, $G = \frac{2}{3}$.

moments were those which made the plots of figure 2 most nearly equal to a constant (obtained by least squares fit), although error incurred from this source is negligible compared with error from the integration scheme itself.

Since this data is not taken to asymptotically large times the moment ratios depend on the integration scheme. The integration schemes used were simple square counting, the trapezoidal rule and Simpson's rule. The square counting scheme and the trapezoidal rule should, on average, yield the same result, since the scaling function is symmetric about $z = 0$ and the square counting scheme overestimates for $z < 0$ and underestimates (by an equal amount) for $z > 0$. The greatest data fluctuations are incurred for the higher moments since differences exist between the even and odd time steps around $z = 0$. There are trade-offs involved with all methods used. Unless some form of interpolation or other numerical approximation scheme is used, Simpson's rule can be used only on the even time steps, since it requires an odd number of data points. This extra numerical approximation will introduce a further source of error which, of course, is undesirable. Therefore in using Simpson's rule one half of the data used in averaging the moments is lost, although the integration scheme itself is a fourth-order method which is to be contrasted with the trapezoidal rule which is a second-order method. A better means of comparing the two integration schemes is to eliminate one half the data when using the trapezoidal rule, even though no such restrictions exist in application of this method. Table 3 contrasts these different results.

The final test of universality is one concerning the experiments obtained from each model. Measures of ratios of the exponents $\gamma/\nu_\parallel - 1$, $\gamma/\nu_\parallel + \nu_\perp/\nu_\parallel - 1$, and $\gamma/\nu_\parallel + 2\nu_\perp/\nu_\parallel - 1$ can be obtained by plotting the log of the nth moment of $G(M^n(t))$ against log time. Such plots for square bond percolation are shown in figure 6. By least squares fitting these data to straight lines, the ratios $(\gamma/\nu_\parallel) + n(\nu_\perp/\nu_\parallel) - 1$ are obtained from moment n. The results for $n = 0$ for all models and those obtained by other authors are shown in table 1. The errors quoted in our data result from binning the data into 50 bins of 1000 runs each. This error analysis has been discussed earlier in this paper. A plot of the exponent ratio $(\gamma/\nu_\parallel) - 1$ and the respective error bars for several models appear in figure 7.

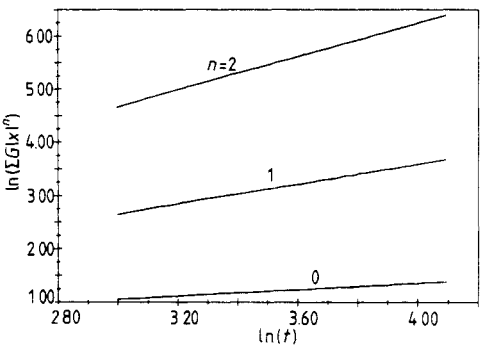

Figure 6. Plots of $\log M^{(n)}(t)$ against $\log t$ for square bond percolation.

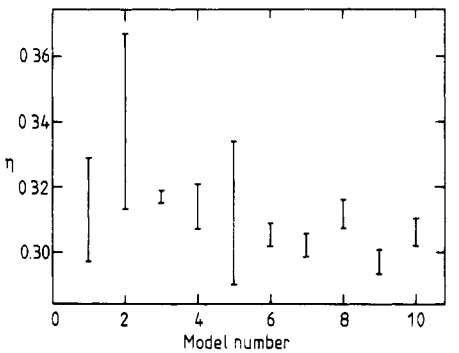

Figure 7. Plots of $\eta(\eta = \gamma/\nu_\parallel - 1)$ for several models showing error bars. These models correspond to: (1) Blease (1977b) square bond, (2) Blease (1977b) triangular bond, (3) Brower *et al* (1978) RQS, (4) Grassberger and De La Torre (1979) RFT, (5) De'Bell and Essam (1983) square bond, (6) square bond, (7) triangular bond, (8) square site, (9) triangular site, (10) square site–bond.

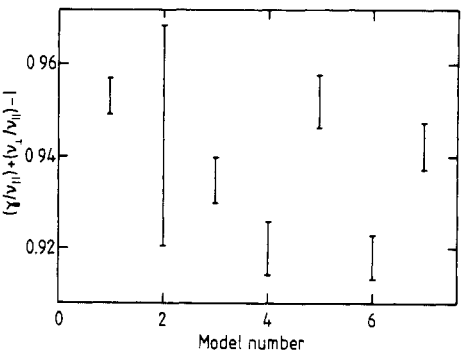

Figure 8. Plots of $(\gamma/\nu_\parallel) + (\nu_\perp/\nu_\parallel) - 1$ for several models showing error bars. These models correspond to: (1) Brower *et al* (1978) RQS, (2) De'Bell and Essam (1983) square bond, (3) square bond, (4) triangular bond, (5) square site, (6) triangular site, (7) square site–bond.

4. Conclusions

We have generated Monte Carlo data for directed percolation on five types of 2D lattices. From this data we have tested scaling by plotting Φ and its nth moment at

several different times. These results are shown in figures 4 and 2 respectively. This data readily demonstrates that scaling is obeyed for $t \geqslant 20$.

By comparing ratios of the moments of Φ we have also tested universality in this work. The results are given in table 3. Although these ratios differ from model to model by about 5%, we still believe that this is a good indication that universality is correct.

Finally, we have tested the universality of the exponent ratios $(\gamma/\nu_\parallel)+n(\nu_\perp/\nu_\parallel)-1$ for $n=0, 1, 2$ by plotting the log of the nth moment of G against log time as in figure 6. The resulting exponent ratios obtained are shown in figure 7 and are also given in table 1 for $n=0$. For the five models tested we find that

$$(\gamma/\nu_\parallel)-1=0.305\pm0.007 \tag{4.1}$$

where the uncertainty represents a measure of the fact that the exponent values for the two site models lie outside each others respective error bars. If we can assume that for some reason the systematic errors incurred in the site model are much larger than in the other models, then we certainly get consistency and find that

$$(\gamma/\nu_\parallel)-1=0.304\pm0.004. \tag{4.2}$$

This result is consistent with the quoted error bars of other workers (see figure 7) but is inconsistent with the results of Brower *et al* (1978). One possible reason is that corrections to scaling may be more important in their work since they do not work at asymptotically large times.

Similarly from the first and second moments we find

$$(\gamma/\nu_\parallel)+(\nu_\perp/\nu_\parallel)-1=0.933\pm0.010 \tag{4.3}$$

and

$$(\gamma/\nu_\parallel)+2(\nu_\perp/\nu_\parallel)-1=1.562\pm0.016 \tag{4.4}$$

respectively. Subtracting the result of the zeroth moment from that of the first moment we find

$$(\nu_\perp/\nu_\parallel)=0.629\pm0.010. \tag{4.5}$$

This result is compared with other workers in figure 9.

As stated in the introduction, lines of constant G provide the shape of a typical cluster. As shown in figure 10 these clusters do not appear to close on the origin for small G. For sites on the light cone ($|x|=t$), G is given analytically by

$$G=\exp(-t/l) \tag{4.6}$$

where $l\equiv 1/|\ln p_c|$. Therefore the boundaries of the cluster on the light cone can be found for a given G. This typical cluster shape compares with that given by Kertesz and Vicsek (1980).

Since it is difficult to attribute the systematic errors in this work to one particular source, more conclusive results might be obtained from Monte Carlo studies such as this one if several effects are taken into account. For example, by increasing the maximum number of time steps (T) used in the lattice simulation the errors incurred due to corrections to scaling would be further reduced, and statistical fluctuations may be further reduced, since this would provide more data over which the average moments $\chi^{(n)}$ could be taken. Secondly, for a given t, the number of values of x and therefore z is given by $t+1$. Therefore in evaluating the moments of Φ, greater t implies a

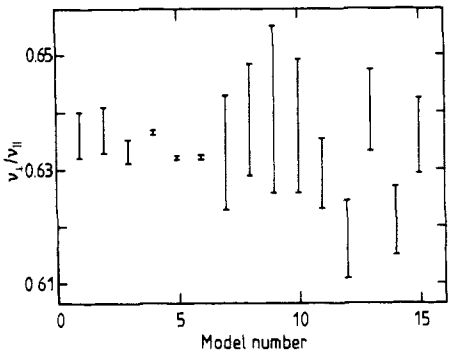

Figure 9. Plots of $(\nu_\perp/\nu_\parallel)$ for several models showing error bars. The models correspond to: (1) Brower *et al* (1978) RQS, (2) Grassberger and De La Torre (1979) RFT, (3) De'Bell and Essam (1981) square bond, (4) Kinzel and Yeomans (1981) square site, (5) Kinzel and Yeomans (1981) square bond, (6) Kinzel and Yeomans (1981) square site–bond, (7) De'Bell and Essam (1983) square bond, (8) De'Bell and Essam (1983) square site, (9) De'Bell and Essam (1983) triangular bond, (10) De'Bell and Essam (1983) triangular site, (11) square bond, (12) triangular bond, (13) square site, (14) triangular site, (15) square site–bond.

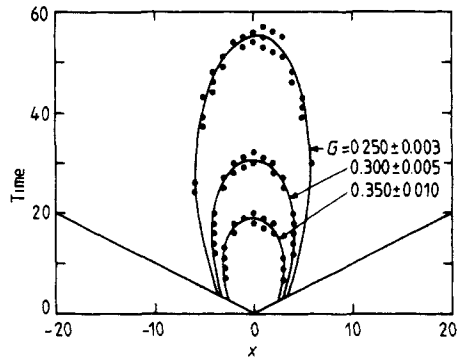

Figure 10. Lines of constant G. Note that the scale has been expanded in the x direction to show the shape of the clusters better.

greater number of data points involved in the integration, and therefore (in principle) a greater accuracy.

Another source of systematic error which might be present in our data is the choice of the lower bound for least squares fitting. However, by increasing the lower bound over which the least squares fit is performed and thereby decreasing possible systematic correction to scaling errors, one induces more error in the slope of the fitted line.

The one outstanding difficulty with this increase in data is that a significant increase in the amount of CPU time would be required for larger lattice and ensemble sizes. Larger lattice size (T) requires more calculations to be performed (the number of calculations goes roughly as the number of time steps (T) squared), and a larger ensemble size (N) would be required to ensure that the data obtained at these large times has an acceptably small fractional error (the number of runs in the ensemble required to produce a single event along lines of constant Φ goes down as a power law with increasing time).

It must be noted that the programs used to generate this data were the simplest ones possible. By improving the algorithm used significant decreases in the amount of CPU time could be made. Such improvements are possible in storage of the data which gets passed in different subroutines. Also, importance sampling can be used to further decrease statistical errors and thus decrease the amount of CPU time.

Acknowledgments

I wish to thank J Cardy for his many helpful comments and the National Science Foundation for the support provided under Grant No PHY 80-18938.

References

Abarbanel H D I, Bronzan J B, Schwimmer A and Sugar R L 1976 *Phys. Rev.* D **14** 632
Amati D, Ciafaloni M, Le Bellac M and Marchesini G 1976 *Nucl. Phys.* B **112** 107
Blease J 1977a *J. Phys. C: Solid State Phys.* **10** 917
—— 1977b *J. Phys. C: Solid State Phys.* **10** 3461
Brower R C, Furman M A and Moshe M 1978 *Phys. Lett.* **76B** 213
Cardy J L and Sugar R L 1980 *J. Phys. A: Math. Gen.* **13** L423
Dhar D and Barma M 1981 *J. Phys. C: Solid State Phys.* **14** L1
Essam J W and De'Bell K 1981 *J. Phys. A: Math. Gen.* **14** L459
—— 1983 *J. Phys. A: Math. Gen.* **16** 385
Grassberger P and De La Torre A 1979 *Ann. Phys., NY* **122** 373
Griffeath D 1979 *Springer lecture notes in Mathematics* vol 724
Kertesz J and Vicsek T 1980 *J. Phys. C: Solid State Phys.* **13** L343
Kinzel W and Yeomans J M 1981 *J. Phys. A: Math. Gen.* **14** L163
Murray B G 1979 *Population Dynamics* (New York: Academic)
Schlögl F 1972 *Z. Phys.* **253** 147